



HAL
open science

Imaging the impact of blood-brain barrier disruption induced by focused ultrasound on P-glycoprotein function

Sébastien Goutal, Anthony Novell, Sarah Leterrier, Louise Breuil, Erwan Selingue, Matthieu Gerstenmayer, Solène Marie, Bruno Saubaméa, Fabien Caillé, Oliver Langer, et al.

► **To cite this version:**

Sébastien Goutal, Anthony Novell, Sarah Leterrier, Louise Breuil, Erwan Selingue, et al.. Imaging the impact of blood-brain barrier disruption induced by focused ultrasound on P-glycoprotein function. *Journal of Controlled Release*, 2023, 361, pp.483-492. 10.1016/j.jconrel.2023.08.012 . hal-04254542

HAL Id: hal-04254542

<https://hal.science/hal-04254542>

Submitted on 23 Oct 2023

HAL is a multi-disciplinary open access archive for the deposit and dissemination of scientific research documents, whether they are published or not. The documents may come from teaching and research institutions in France or abroad, or from public or private research centers.

L'archive ouverte pluridisciplinaire **HAL**, est destinée au dépôt et à la diffusion de documents scientifiques de niveau recherche, publiés ou non, émanant des établissements d'enseignement et de recherche français ou étrangers, des laboratoires publics ou privés.

1 **Imaging the impact of blood-brain barrier disruption induced by focused ultrasound**
2 **on P-glycoprotein function**

3 Sébastien Goutal¹, Anthony Novell¹, Sarah Leterrier¹, Louise Breuil^{1,2}, Erwan Selingue³,
4 Matthieu Gerstenmayer³, Solène Marie¹, Bruno Saubaméa², Fabien Caillé¹, Oliver Langer⁴,
5 Charles Truillet¹, Benoît Larrat³, Nicolas Tournier^{1,*}

6
7 ¹ Laboratoire d'Imagerie Biomédicale Multimodale (BioMaps), Université Paris-Saclay, CEA,
8 CNRS, Inserm, Service Hospitalier Frédéric Joliot, 4 place du Général Leclerc, 91401,
9 ORSAY France.

10 ² Université Paris Cité, Inserm, UMRS-1144, Optimisation Thérapeutique en
11 Neuropsychopharmacologie, 75006 Paris, France

12 ³ Neurospin, Institut Joliot, Direction de la Recherche Fondamentale, CEA, Université Paris
13 Saclay, Gif sur Yvette, France

14 ⁴ Department of Clinical Pharmacology, Medical University of Vienna, Vienna, Austri

15

16 ***Corresponding author:**

17 Nicolas TOURNIER

18 CEA/SHFJ, 4 place du Général Leclerc 91400 ORSAY, France

19 nicolas.tournier@cea.fr

20

21 **Declaration of interest:** None.

22 **Color for figures in print:** Yes

23

24 **Keywords:** Blood-brain barrier integrity, brain delivery, efflux transporter, membrane
25 transporters, therapeutic ultrasound.

26

27

28

29

30

31

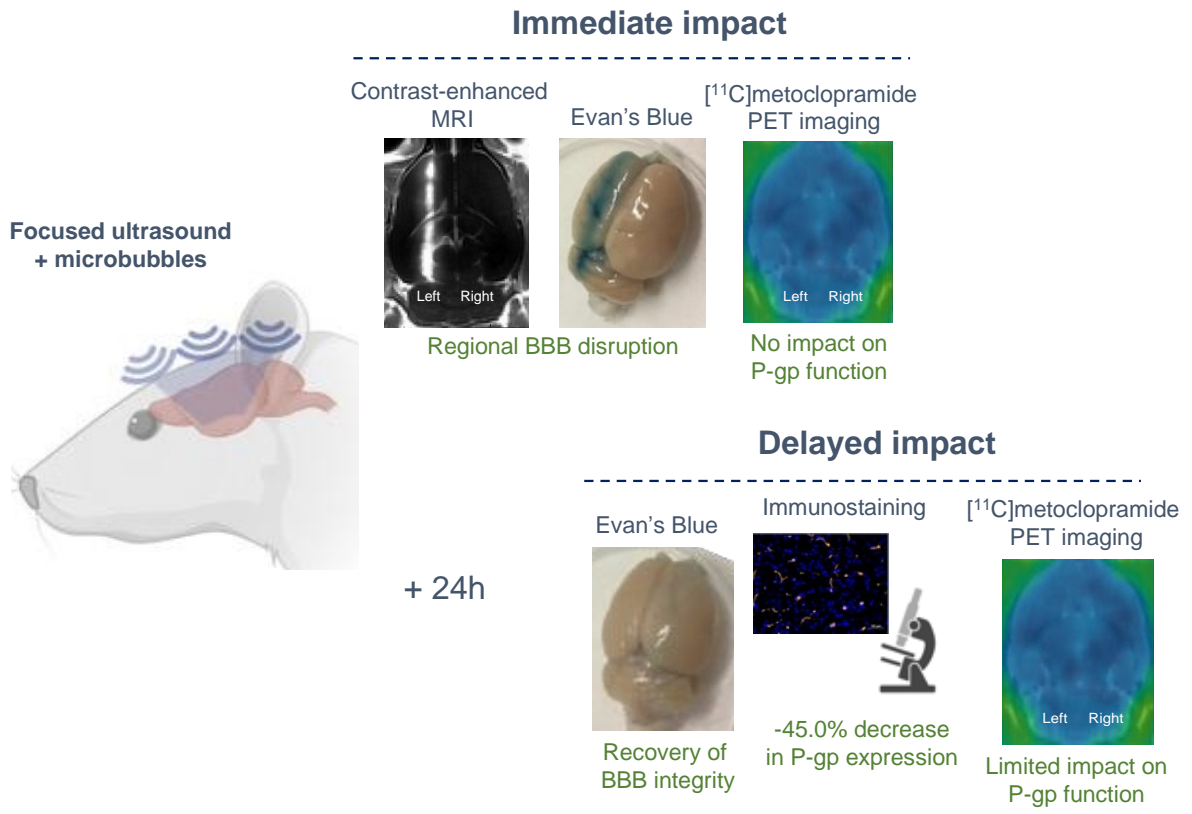
1 **Highlights**

- 2 • P-glycoprotein (P-gp) hinders the blood-brain barrier (BBB) passage of many drugs
- 3 • BBB disruption induced by focused ultrasound (FUS) enables targeted brain delivery
- 4 • P-gp function at the BBB can be studied in vivo using [¹¹C]metoclopramide PET
- 5 imaging
- 6 • Immediately after FUS, BBB disruption did not impact the P-gp-mediated efflux in rats
- 7 • P-gp expression was decreased 24h to 48 h after FUS, with limited impact on function

8

1 **Graphical Abstract**

2
3



4
5
6

1 **Abstract (350 words)**

2 The P-glycoprotein (P-gp/ABCB1) is a major efflux transporter which impedes the brain
3 delivery of many drugs across the blood-brain barrier (BBB). Focused ultrasound with
4 microbubbles (FUS) enables BBB disruption, which immediate and delayed impact on P-gp
5 function remains unclear. Positron emission tomography (PET) imaging using the
6 radiolabeled substrate [¹¹C]metoclopramide provides a sensitive and translational method to
7 study P-gp function at the living BBB.

8 A FUS protocol was devised in rats to induce a substantial and targeted disruption of the
9 BBB in the left hemisphere. BBB disruption was confirmed by the Evan's Blue extravasation
10 test or the minimally-invasive contrast-enhanced MRI. The expression of P-gp was measured
11 24h or 48h after FUS using immunostaining and fluorescence microscopy. The brain kinetics
12 of [¹¹C]metoclopramide was studied by PET at baseline, and both immediately or 24h after
13 FUS, with or without half-maximum P-gp inhibition (**tariquidar** 1 mg/kg). In each condition
14 (n=4-5 rats per group), brain exposure of [¹¹C]metoclopramide was estimated as the area-
15 under-the-curve (AUC) in regions corresponding to the sonicated volume in the left
16 hemisphere, and the contralateral volume. Kinetic modeling was performed to estimate the
17 uptake clearance ratio (**R₁**) of [¹¹C]metoclopramide in the sonicated volume relative to the
18 contralateral volume.

19 In the absence of FUS, half-maximum P-gp inhibition increased brain exposure
20 (+135.0±12.9%, p<0.05) but did not impact R₁ (p>0.05). Immediately after FUS, BBB integrity
21 was selectively disrupted in the left hemisphere without any detectable impact on the brain
22 kinetics of [¹¹C]metoclopramide compared with the baseline group (p>0.05) or the
23 contralateral volume (p>0.05). 24h after FUS, BBB integrity was fully restored while P-gp
24 expression was maximally down-regulated (-45.0±4.5%, p<0.001) in the sonicated volume.
25 This neither impacted AUC nor R₁ in the FUS+24h group (p>0.05). Only when P-gp was
26 inhibited with tariquidar were the brain exposure (+130±70%) and R₁ (+29.1±15.4%)
27 significantly increased in the FUS+24h/**tariquidar** group, relative to the baseline group
28 (p<0.001).

29 We conclude that the brain kinetics of [¹¹C]metoclopramide specifically depends on P-gp
30 function rather than BBB integrity. Delayed FUS-induced down-regulation of P-gp function
31 can be detected. Our results suggest that almost complete down-regulation is required to
32 substantially enhance the brain delivery of P-gp substrates.

33
34
35
36
37

1
2
3
4
5
6
7
8
9
10
11
12
13
14
15
16
17
18
19
20
21
22
23
24
25
26
27
28
29
30
31
32
33
34
35
36
37

Introduction

The blood-brain barrier (BBB) is a complex and dynamic biological interface [1]. The BBB is primarily supported by endothelial cells forming the inner surface of brain microvessels [2]. The “physical” BBB mainly results from tight-junctions between adjacent endothelial cells, which reduce paracellular (between cells) passage of solutes and force most molecular traffic to take a transcellular route (across cells) [3]. The “functional” BBB mainly relies on the activity of membrane transporters that selectively control the transcellular traffic of endogenous and exogenous compounds, thus regulating brain homeostasis and protecting the brain from potentially harmful substances in circulating blood [2,4].

The P-glycoprotein (P-gp, ABCB1) is the most studied efflux transporter at the BBB. P-gp belongs to the ATP-binding cassette superfamily which restricts the brain exposure to many structurally unrelated substrates including endogenous compounds and xenobiotics [5,6]. Complementarity between the physical and the functional BBB limits the ability of most drugs to naturally reach the brain parenchyma and exert CNS effects [2]. **Drugs whose brain penetration is selectively hindered by P-gp include, for instance, antimicrobial agents such as itraconazole [7], abacavir or nelfinavir [8], as well as anticancer drugs such as paclitaxel, docetaxel, vinblastine and many others [9]. As a consequence, the BBB is a bottleneck for the development of new drugs for the treatment of CNS diseases, and many drug candidates are abandoned due to P-gp-mediated efflux at the BBB [10–12].**

Focused ultrasound associated with microbubbles (FUS) provides a unique method to enable localized and transient disruption of the physical BBB, in animals and patients [13]. FUS is increasingly envisioned to enhance the brain delivery of various drugs with the aim to treat various CNS diseases with drugs which do not naturally cross the physical BBB [14]. However, there is a scarcity of data regarding the impact of FUS on the expression and functionality of the P-gp, as well as the consequences of FUS on the brain delivery of P-gp substrates. Some studies suggest that the BBB passage of some P-gp substrates may predominantly depend on P-gp function rather than the physical integrity of the BBB [15,16]. Other studies have consistently reported a significant decrease in the expression of P-gp at the BBB from 24h to 48h after FUS [17–20]. **However, it remains to be evaluated whether delayed FUS-induced down-regulation of the P-gp may locally enhance the brain delivery of P-gp substrates. This would provide a versatile means to overcome either the physical or the functional BBB, taking advantage of either the immediate or the delayed effects of FUS.**

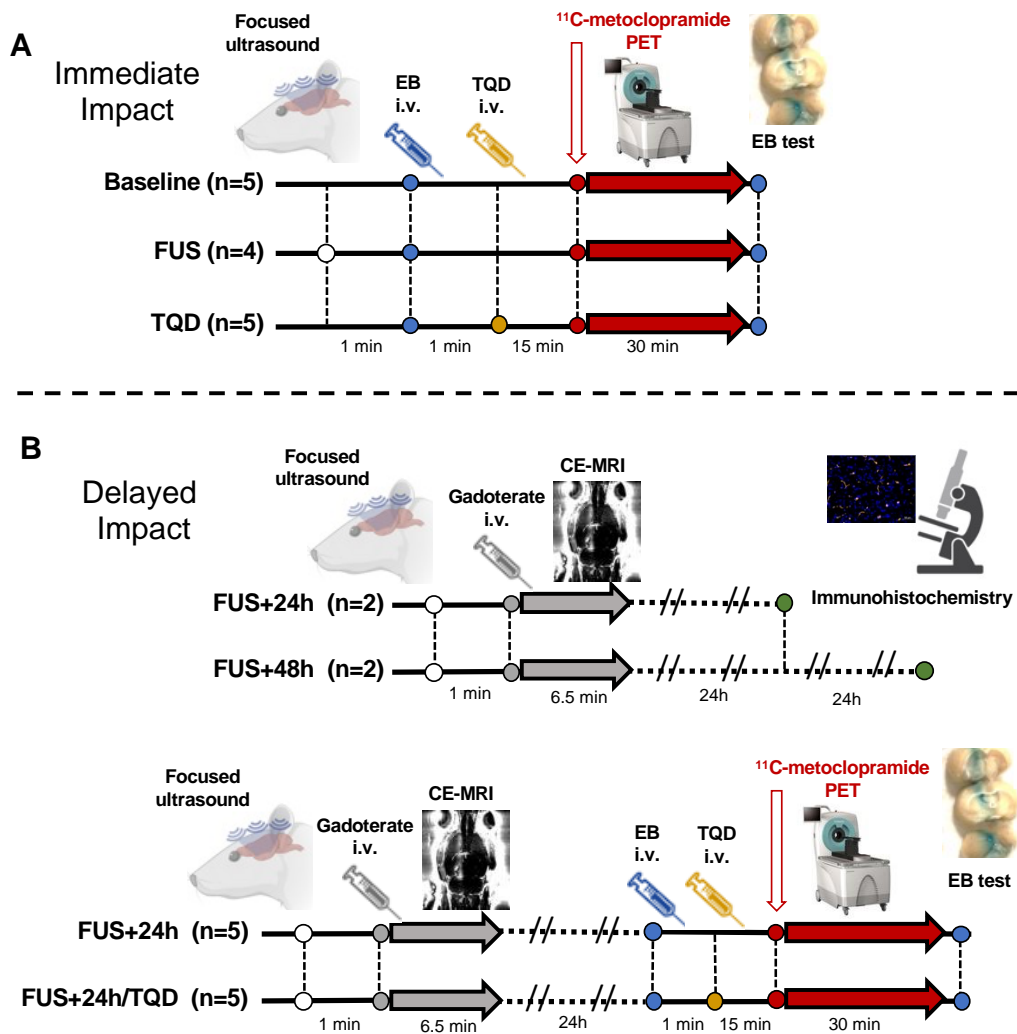
Minimally-invasive methods are needed to investigate the immediate and delayed impact of FUS on the brain delivery of therapeutics. In this framework, Positron Emission Tomography (PET) imaging using radiolabeled compounds provides a translational technique for quantitative determination of FUS-aided brain delivery of a large variety of compounds,

1 including small molecules and biologics [21–24]. Among available PET probes to estimate P-
2 gp function at the BBB, [¹¹C]metoclopramide benefits from selectivity for P-gp [25], high
3 sensitivity to detect changes in P-gp function [26,27], ability to detect an induction of P-gp
4 function at the BBB [28] and a successful transfer to humans [29].
5 In the present study, the immediate and delayed impact of FUS-induced BBB disruption on
6 P-gp function was assessed using [¹¹C]metoclopramide PET imaging in rats. An optimized
7 FUS protocol was applied to rats to induce a transient and spatially-controlled disruption of
8 the BBB. [¹¹C]metoclopramide PET imaging was performed during BBB disruption (i.e.
9 immediately after FUS) and 24h after FUS. PET data were interpreted in the light of different
10 markers of BBB integrity and expression of P-gp in the sonicated brain volume.
11

1 **Material and methods**

2 *Study design*

3 [¹¹C]Metoclopramide PET imaging and assessment of BBB integrity using Evan's Blue (EB)
4 extravasation test were simultaneously performed. Immediately before PET acquisition, all
5 animals received an **intravenous (i.v)** injection of EB and extravasation was visually
6 assessed on the resected brain, immediately after PET acquisition (Fig. 1).
7 [¹¹C]Metoclopramide PET imaging + EB was performed in control animals, in the absence of
8 any intervention on BBB integrity or function (Baseline group, n=5 rats). To assess the acute
9 impact of BBB disruption or functional inhibition, [¹¹C]Metoclopramide PET imaging + EB
10 were performed immediately after FUS (FUS group, n=4), or after P-gp inhibition with
11 tariquidar (TQD group, n=5) respectively [25]. The selected dose of TQD (1 mg/kg; i.v) was
12 previously shown to inhibit 50% of the P-gp mediated transport of [¹¹C]metoclopramide at the
13 BBB [26] (Fig. 1).



14

15 **Fig. 1 Study design**

16 In A, the immediate impact of blood-brain barrier (BBB) disruption induced by focused ultrasound
17 (FUS) on P-glycoprotein (P-gp) function was assessed using [¹¹C]metoclopramide in rats, and

1 compared with partial (~50%) P-gp inhibition achieved using tariquidar (TQD, 1 mg/kg). In B, the
2 delayed impact of FUS on P-gp expression was assessed using immunohistochemistry (24h and 48h
3 after FUS). The functional impact was tested 24h after FUS in the absence and the presence of partial
4 P-gp inhibition. Integrity of the BBB in terms of paracellular transport was tested using either the
5 Evan's blue (EB) extravasation test or contrast-enhanced magnetic resonance imaging (CE-MRI).

6
7 To assess the delayed impact of BBB disruption, effective BBB disruption was assessed
8 immediately after FUS using minimally invasive contrast-enhanced magnetic resonance
9 imaging (CE-MRI). Expression of P-gp was measured by quantitative fluorescence
10 microscopy of immunostained rat brain sections 24h and 48h after FUS (n=2 rats per time
11 point). Brain [¹¹C]metoclopramide PET imaging + EB was performed 24h after FUS-induced
12 BBB disruption, without (FUS+24h, n=5 rats) or with concurrent half-maximum P-gp inhibition
13 (FUS+24h/TQD, n=5 rats).

14 *Chemistry / Radiochemistry*

15 Tariquidar used for P-gp inhibition was purchased from Eras Labo (France). Tariquidar
16 solutions for intravenous injection (4.4 mg·mL⁻¹) were freshly prepared on the day of the
17 experiment by dissolving tariquidar dimesylate in dextrose solution (5%, w/v), followed by
18 dilution with sterile water [25]. EB was obtained from Sigma-Aldrich (France).

19 Ready-to-inject [¹¹C]metoclopramide, was prepared as previously described [30] starting from
20 cyclotron-produced [¹¹C]carbon dioxide (Cyclone-18/9 cyclotron; IBA, Belgium) by O-
21 [¹¹C]methylation of nor-metoclopramide (Toronto Chemicals, Canada), using a TRACERLab
22 FX CPro synthesizer (GE Healthcare, France). Quality control was performed by radio-high-
23 performance liquid chromatography (HPLC) to assess the identity, radiochemical and
24 chemical purity and the molar activity of the radiotracer.

25 *Animals*

26
27 A total of 28 male Sprague Dawley rats (Janvier, France) were used for the study (mean
28 weight: 275.9±20.4 g). **Animals were housed and acclimatized for at least 3 days before
29 experiments. Rats were housed under standard experimental conditions: room temperature
30 (20 ± 2°C); light/dark cycle (14 h light/10 h dark); free access to water and food (pellets) *ad
31 libitum*. Rats were kept in social groups of two rats per cage. Polycarbonate shelters and
32 wooden tubes have been added in the cages for enrichment. All interventions on animals
33 were performed under isoflurane anesthesia (2-2.5% isoflurane in a mixture of air/O₂; 50/50,
34 v/v).**

35
36 All animal experiments were in accordance with the recommendations of the European
37 Community (2010/63/UE) and the French National Committees (law 2013-118) for the care

1 and use of laboratory animals. The experimental protocol was approved by a local ethics
2 committee for animal use (CETEA) and by the French ministry of agriculture
3 (APAFIS#16293-2018072609593031/Ethics committee n°44). Samples size for each group
4 was based on previous studies [25,26]. Reporting of animal data is in compliance with the
5 ARRIVE (Animal Research: Reporting in Vivo Experiments) guidelines.

6 7 *Focused ultrasound*

8 Transient disruption of BBB integrity was adapted from a previously published FUS protocol
9 designed to induce a large and controlled “line”-shaped BBB disruption in rats in one brain
10 hemisphere of rats [21]. The ultrasound set up consisted in a single element concave
11 transducer (diameter of 25 mm, focal depth 20 mm, Imasonic, France) with a central
12 frequency of 1.5 MHz. The transducer was connected to a single channel generator
13 synchronized with a motorized XYZ stage (CUBE, Image Guided Therapy, France). **The**
14 **CUBE system includes a sine wave generator, a 50 W amplifier and a degasser to remove**
15 **air bubbles trapped into the water-filled balloon. The XYZ motorized stage is also driven by**
16 **the CUBE system using the BBBop software (Image Guided Therapy), allowing for**
17 **synchronous transmission of FUS with transducer displacement.** The delivered acoustic
18 pressure was estimated using a 200- μ m calibrated hydrophone (HGL-0200, preamplifier AH-
19 2020, Onda Corporation, USA) mounted on a micrometric 3D positioning stage and
20 positioned at the focus of the transducer in a water tank. **The -6dB focal dimensions of the**
21 **sound beam are 7 mm (axial) and 1 mm (lateral).**

22 Rats were installed in prone position on a dedicated bed into a stereotactic frame. The
23 transducer holder was fixed on a rail allowing reproducible head-foot displacement over a
24 line permitting targeted sonication of the left-brain hemisphere of the animals. The transducer
25 was coupled to the shaved head of the animals with a latex balloon filled with deionized and
26 degassed water. Acoustic gel was applied to the skin in order to ensure efficient coupling
27 with the balloon. A 200 μ L bolus of commercially available microbubbles (SonoVue[®], Bracco,
28 Italy) was injected i.v.. Ultrasound sonication started immediately after microbubble injection,
29 with continuous waves set at an estimated peak negative acoustic pressure of 0.63 MPa *in*
30 *situ* at focus. Ultrasound transmission at 1.5 MHz through the skull was previously estimated
31 to be 42% for a 300 g rat [31]. An amplitude compensation was applied as a function of the
32 animal weight. The transducer was repeatedly moved back and forth above the left
33 hemisphere along a single axis, in a range of 14 mm at a speed of 10 mm/s with 3s repetition
34 cycles. Continuous ultrasound waves were transmitted during 3 minutes.

35 36 *MRI-based evaluation of FUS-induced BBB disruption protocol*

1 For animals of the FUS+24h and the FUS+24h/TQD groups, effective disruption of the BBB
2 was non-invasively checked 24h before [¹¹C]metoclopramide PET imaging + EB. To this end,
3 CE-MRI was performed as previously described [21]. Briefly, rats were i.v injected with
4 gadoterate (200 µL, Dotarem® 0.5 mmol/mL, Guerbet, France) immediately after the FUS
5 protocol. MRI images were acquired using a 7T small-animal MRI scanner (Bruker,
6 Germany). A T1-weighted sequence (Multi Slice Multi Echo, TE/TR = 3/300 ms, spatial
7 resolution = 0.250x0.250x1 mm³, matrix size = 128x128x14, 5 averages, acquisition time =
8 3.12 min) was used to detect the signal enhancement due to the gadolinium chelate
9 delivered into brain tissues.

10

11 *Expression of P-gp in the brain*

12 In additional rat groups, the expression of P-gp in the brain was assessed using fluorescent
13 immunostaining of brain slices taken 24h and 48h after FUS (n=2 rats for each time-point).
14 First, the FUS-induced BBB disruption protocol was applied. The effectiveness of BBB
15 disruption was assessed using CE-MRI, as described above. At either 24h or 48h after FUS,
16 animals were killed. Brains were removed and fresh-frozen using isopentane (-50°C,
17 HoneyWell, USA) and liquid nitrogen (Air Products, France), and stored at -80°C until
18 analysis. The slides with affixed 14-µm thick cryosections of the brain were incubated for 15
19 min at room temperature (rt) in 4% paraformaldehyde (PFA, Sigma-Aldrich), and then for 5
20 min at rt in phosphate-buffered saline PBS containing 50 mM of ammonium chloride (both
21 from Sigma-Aldrich) to quench remaining aldehydes. Sections were permeabilized in frozen
22 methanol/acetone (1/1; v/v 5 min, -20°C, from Carlo Erba Reagents, France) followed by
23 0.1% Triton X100 (Sigma-Aldrich) in PBS (5 min, rt). Three washes with PBS were carried
24 out between each of these steps. The non-specific sites were saturated by incubating the
25 slides for 45 minutes at rt in blocking buffer which consisted in PBS containing 5% Bovine
26 Albumin Serum (Fisher Bioreagents, USA) and 0.5% Tween 80 (Sigma-Aldrich). Each slide
27 was incubated for 1 h, in the presence of P-glycoprotein primary antibody (#MA1-26528,
28 Invitrogen, USA) diluted 1/100 in blocking buffer. After several washes with PBS, the slides
29 were left for 45 minutes at rt in Alexa-Fluor 546 donkey anti-mouse secondary antibody
30 (Invitrogen) diluted 1/1000 in blocking buffer. Finally, slides were rinsed again, then mounted
31 in ProLong™ Diamond Antifade Mountant (Invitrogen) containing 4',6-diamidino-2-
32 phenylindole (DAPI) for labeling the nuclei. Brain sections were observed using a 20x lens of
33 a Zeiss AxioCam fluorescence microscope (Carl Zeiss, Germany). Intensity measurement of
34 the fluorescent signal was performed with the ImageJ software (<https://imagej.nih.gov/ij/>)
35 [32]. Two brain slices per rat were included in the analysis. In each section, the whole
36 fluorescence intensity was corrected for background and measured in twelve areas (0.323
37 µm x 0.323 µm) located i) in the sonicated volume of the left hemisphere, where the BBB

1 was disrupted, and ii) on the contralateral region within the non-sonicated right hemisphere.
2 Fluorescence intensity is expressed as a percentage decrease compared with the
3 contralateral region.

4

5 *[¹¹C]Metoclopramide PET imaging and EB extravasation test*

6 MicroPET acquisitions were performed using an Inveon microPET scanner (Siemens, USA).
7 Anesthesia was induced and then maintained using 3.5% followed by 1.5-2.5% isoflurane in
8 pure oxygen. Thirty-minute dynamic PET scans were acquired, starting with i.v bolus
9 injection of [¹¹C]metoclopramide (38.2 ± 5.7 MBq, 1.0 ± 0.4 μ g), via a catheter inserted in the
10 caudal lateral vein.

11 The EB extravasation test was simultaneously performed to assess the integrity status of the
12 physical BBB during the PET acquisition. To this end, animals were i.v. injected with 2 mL/kg
13 of a 4% EB solution, 1 min after ultrasound exposure and 9 min before [¹¹C]metoclopramide
14 injection. At the end of PET experiments, anesthetized animals were decapitated and the
15 brain was removed from the skull. BBB integrity was determined visually by two independent
16 assayers on the intact freshly excised brain and then on ~5 mm thick coronal gross
17 pathology slices.

18

19 *PET data analysis*

20 PET images were reconstructed with the Fourier rebinning algorithm and the 3-dimensional
21 ordered-subset expectation maximization algorithm (OSEM3D) including normalization,
22 attenuation, scatter, and random corrections. Image analysis and quantification of
23 radioactivity uptake in region of interest were performed using PMOD software (version 3.9;
24 PMOD Technologies, Switzerland). Time–activity curves (TACs) were generated with time
25 frame durations of 1 x 0.25 min, 2 x 0.5 min, 1 x 0.75 min, 4 x 1 min, 1 x 1.5 min, 4 x 2 min, 1
26 x 2.5 min, 2 x 3 min and 1 x 3.75 min. Brain radioactivity was corrected for ¹¹C decay and
27 injected dose and expressed as percentage of injected dose per mL of brain tissue (%ID.mL⁻¹).
28

29 Brain exposure was estimated by calculating the area under the brain TACs from either 0 to
30 10 min (AUC_{10min}) or 0 to 30 min (AUC_{30min}) after radiotracer injection. The AUC ratio of the
31 sonicated volume to the non-sonicated (contralateral) volume (AUCR_{10min} and AUCR_{30min})
32 was also calculated. Kinetic modelling of the PET data was performed using The PKIN
33 module of the PMOD software. The simplified reference tissue model (SRTM) was used to
34 describe the kinetic data of [¹¹C]metoclopramide. In this model, K_1 (in mL.cm⁻³.min⁻¹) is the
35 rate constant for transfer from plasma to free compartment of the region of interest
36 (sonicated volume) and K'_1 (in mL.cm⁻³.min⁻¹) is the rate constant for transfer from plasma to
37 free compartment of the reference region (non-sonicated contralateral volume). The SRTM

1 model only estimates R_1 which describes the ratio of the uptake clearance of
2 [^{11}C]metoclopramide in the sonicated volume relative to the non-sonicated volume ($R_1 =$
3 K_1/K'_1) [33]. To use this model, it was assumed a similar binding potential of
4 [^{11}C]metoclopramide in the sonicated and non-sonicated brain tissue. This assumption is
5 based on previous experiments showing that the brain PET signal corresponds to non-
6 displaceable (non-specific) binding in rats [25].

7

8 *Statistical analysis*

9 For the IHC study, percentage change in P-gp expression relative to the contralateral (non-
10 sonicated) hemisphere was compared using a two-tailed one-sample t -test ($n=4$). Outcome
11 parameters of the PET study were compared between conditions using 2-way ANOVA
12 analysis using the Tukey's post-hoc test. Normality of the residues was checked using the
13 Shapiro-Wilk's test and homoscedasticity using the Bartlett's test. Graphical and statistical
14 analysis were performed using Graphpad[®] Prism software (Version 9, USA).

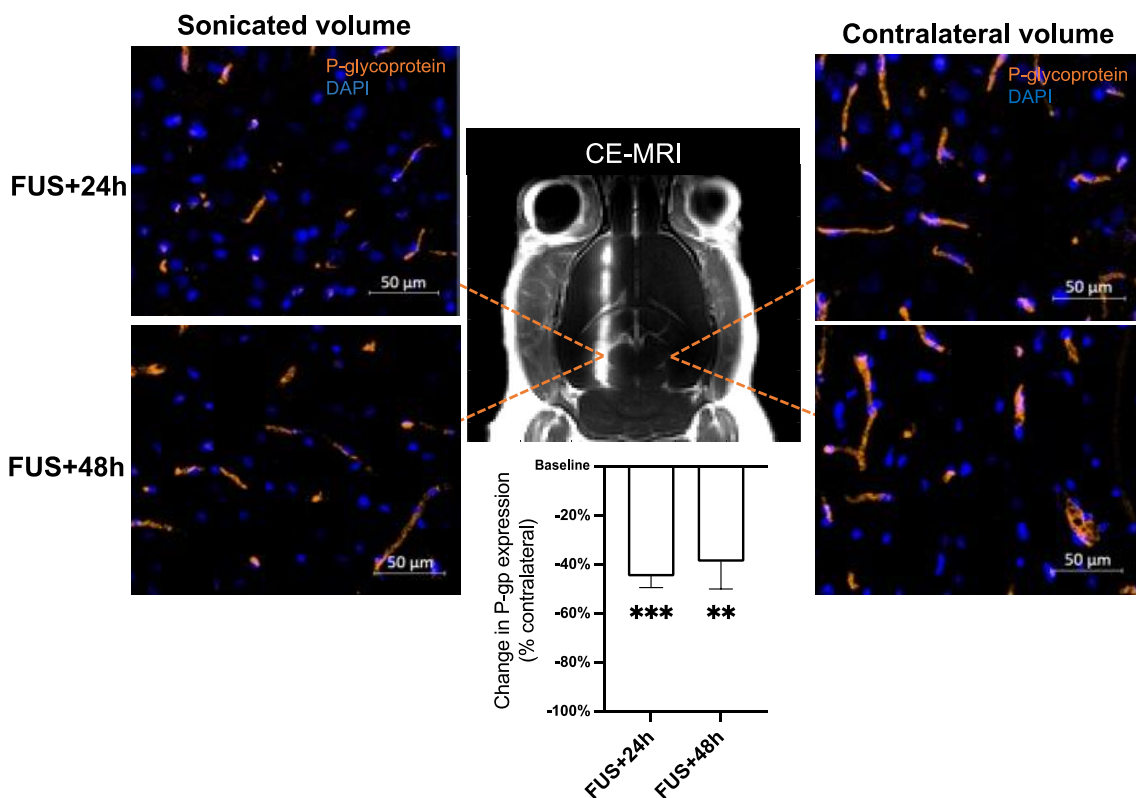
15

1 Results

2 *Impact of FUS on the integrity of the physical BBB*

3 Immediate disruption of the BBB was detected in animals submitted to FUS through either
4 EB extravasation (~40 min after sonication, FUS group) or signal enhancement in CE-MRI
5 (~10 min after sonication, FUS+24h and FUS+24h/TQD groups) (Table 1). EB staining
6 consisted of a large blue stripe located in the left brain hemisphere, in line with previous work
7 using a similar FUS protocol, in which EB extravasation could be observed up to 100 min
8 after sonication [21]. This disruption pattern was confirmed in CE-MRI images, which
9 highlighted a large ~2mm stripe, matching the width of the ultrasound beam, from the front of
10 the brain to the cerebellum (Fig. 2). No signal enhancement could be observed in the
11 mirrored volume drawn in the right hemisphere, thus confirming BBB integrity in the non-
12 sonicated volume. Importantly, no EB extravasation was observed in either the baseline or
13 the TQD groups suggesting an intact BBB in these non-sonicated animals, regardless of P-
14 gp activity. Moreover, no EB extravasation was observed in the FUS+24h and
15 FUS+24h/TQD groups, suggesting full recovery of the BBB integrity at the time of PET
16 acquisition, i.e at 24h after FUS (Table 1).

17



18

19 **Fig. 2. Expression of P-glycoprotein in the sonicated and the non-sonicated (contralateral)**
20 **brain volume determined using immunostaining at 24h (FUS+24h) and 48h (FUS+48h) after**
21 **blood-brain barrier (BBB) disruption induced by focused ultrasound (FUS). BBB disruption was**
22 **assessed using contrast-enhanced MRI (CE-MRI). Expression of P-gp was determined using**

1 immunostaining and fluorescence microscopy and expressed as the percentage of fluorescence
 2 intensity change relative to the contralateral (non-sonicated) volume. DAPI = 4',6-diamidino-2-
 3 phenylindole. Significant change in P-gp expression was tested using a one sample t-test, mean \pm
 4 S.D, n=4 slides from 2 different rats per time point) is shown as **p<0.01, ***p<0.001.

5
6

7 **Table 1.** Assessment of blood-brain barrier (BBB) integrity using either the Evan's blue
 8 extravasation test (EB) or contrast-enhanced magnetic resonance imaging (CE-MRI) in the
 9 different tested conditions. EB was performed either 47 min after FUS (immediate impact), or
 10 24h after FUS (delayed impact). CE-MRI was performed 1 min after FUS. Effective BBB
 11 disruption in the sonicated area is shown as "+", intact BBB is shown as "-".

12

Condition	Immediate impact of FUS		Delayed impact (24h after FUS)
	EB	CE-MRI	EB
Baseline (n=5)	-		
FUS (n =4)	+		
TQD (n=5)	-		
FUS+24h (n=5)		+	-
FUS+24h/TQD (n=5)		+	-

13
14

15 *FUS-induced down-regulation of P-gp expression*

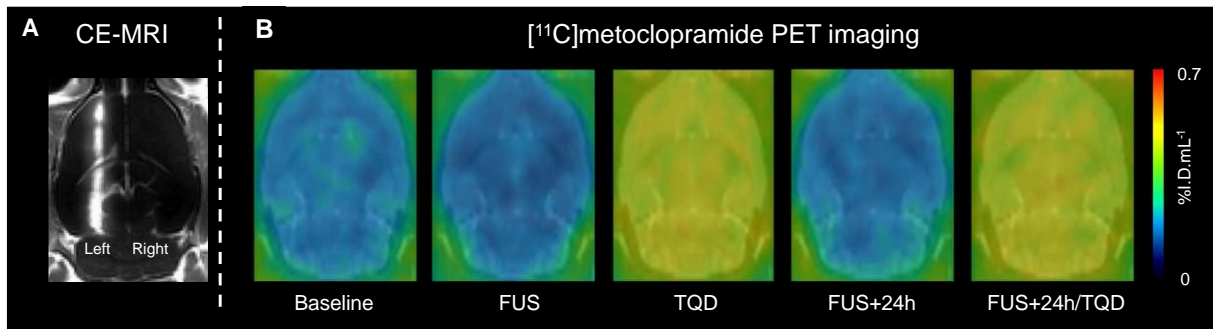
16 P-gp expression in the sonicated brain volume was significantly decreased at both 24h
 17 (p<0.001) and 48h (p<0.001) after FUS compared with the contralateral (non-sonicated)
 18 brain volume (Fig. 2). The decrease in P-gp expression was $-45.0\pm 4.5\%$ at 24h and
 19 $-39.0\pm 11.1\%$ at 48h after FUS (Fig. 2). This is consistent with the dynamics of FUS-induced
 20 down-regulation of brain P-gp described in the literature [17–19].

21

22 *[¹¹C]Metoclopramide PET imaging*

23 Visually, PET images (summed over 0-30 min) observed in the FUS or the FUS+24h group
 24 were similar to baseline PET images. As expected, following P-gp inhibition with tariquidar,
 25 higher PET signal was observed in the TQD and FUS+24h/TQD groups compared with other
 26 groups. No difference could be observed between the sonicated (left) and non-sonicated
 27 (right) hemisphere in any tested group (Fig. 3).

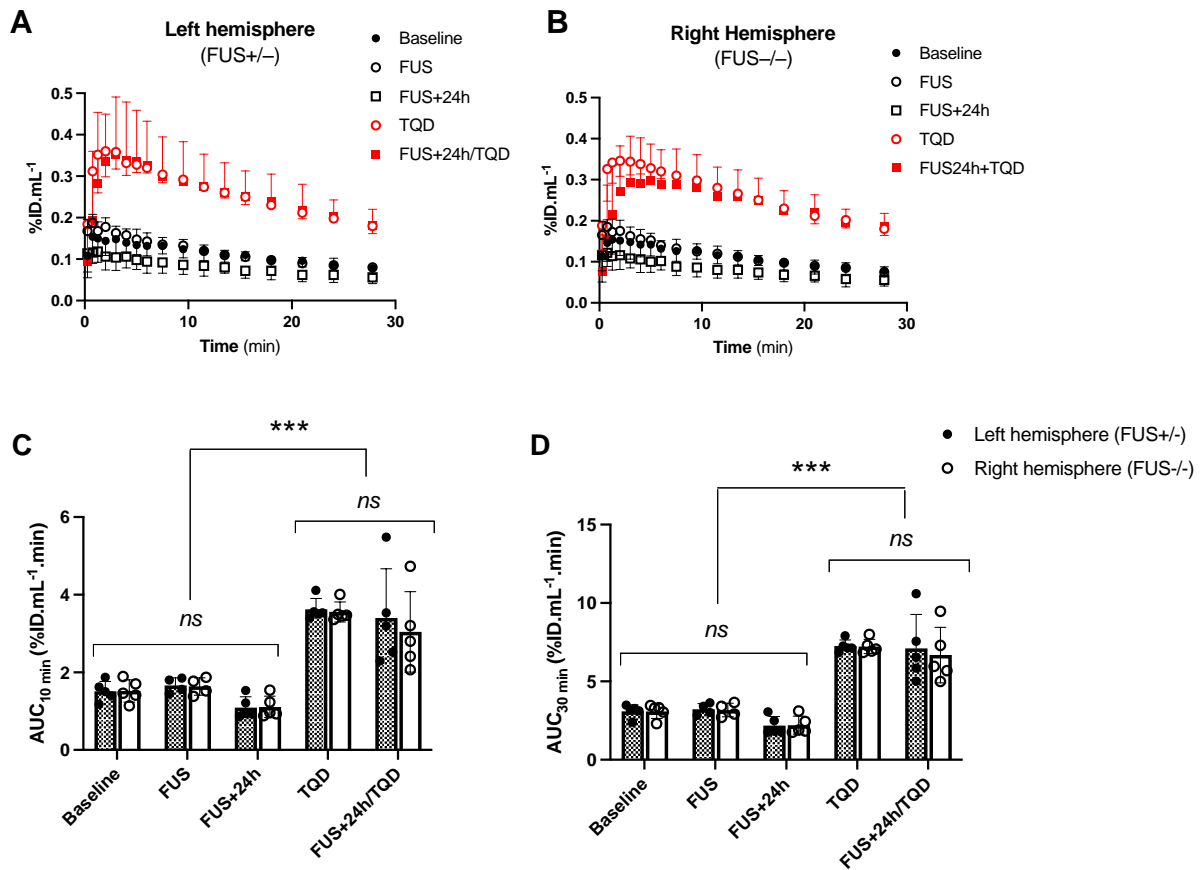
28
29
30



1
 2 **Fig. 3. Impact of regional blood-brain barrier (BBB) disruption induced by focused ultrasound**
 3 **(FUS) on the brain distribution of [¹¹C]metoclopramide.** The localization of the area of BBB
 4 disruption is shown in A, in a representative contrast enhanced MR image. Panel B shows
 5 representative [¹¹C]metoclopramide brain PET summation images (0-30 min) obtained in baseline
 6 condition, immediately after FUS (FUS), after P-gp inhibition using tariquidar (TQD), at 24h after FUS
 7 without (FUS+24h) or with P-gp inhibition (FUS+24h/TQD). Shown are summed PET images (0-
 8 30min).

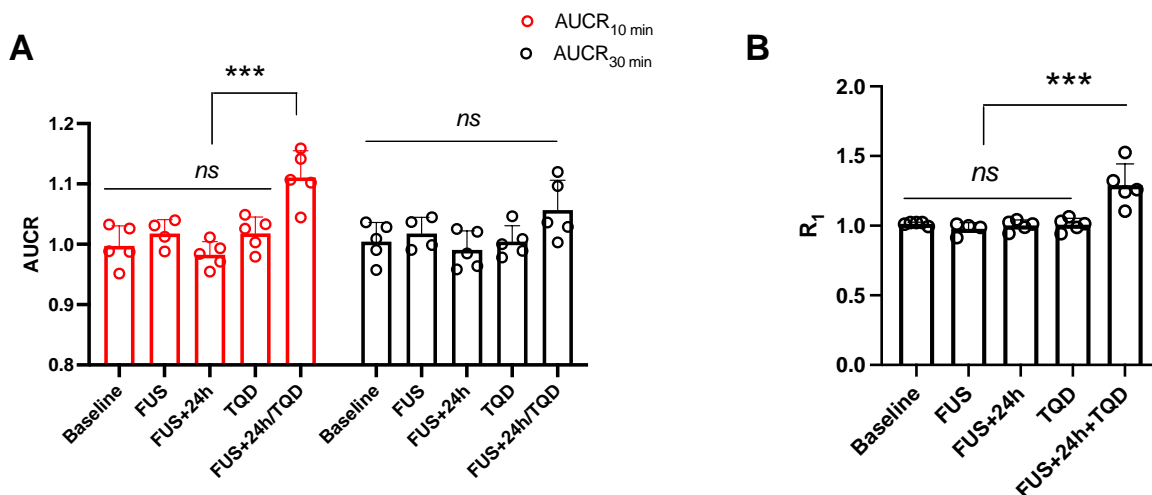
9
 10 PET quantification revealed that BBB disruption alone (FUS group), as confirmed using the
 11 EB test in the FUS group, had no immediate impact on the brain distribution of
 12 [¹¹C]metoclopramide in the sonicated volume (AUC) as compared with non-sonicated
 13 animals of the baseline group ($p > 0.05$; Fig. 4) or on the left/right AUC ratio (AUCR_{10min} or
 14 AUCR_{30min}) of [¹¹C]metoclopramide ($p > 0.05$, Fig. 5). Similar observations were made 24h
 15 following FUS since [¹¹C]metoclopramide PET data obtained in the FUS+24h group showed
 16 no change in the brain exposure (AUC) nor AUCR compared with the baseline group
 17 ($p > 0.05$). Therefore FUS alone is unable to significantly change the brain exposure of
 18 [¹¹C]metoclopramide either immediately, when BBB is disrupted, or 24h later, when BBB
 19 integrity is restored but P-gp expression is reduced.

20



1
 2 **Fig. 4. Brain kinetics of [¹¹C]metoclopramide PET data in the sonicated brain region relative to**
 3 **the contralateral volume.** The ratio of brain exposure expressed as AUCR obtained from 0 to 10 min
 4 (AUCR_{10 min}) or from 0 to 30 min (AUCR_{30 min}) is shown in A. The uptake clearance ratio in the
 5 sonicated brain region relative to the contralateral hemisphere, expressed as R₁, is shown in B. Data
 6 were acquired either at baseline (n=5), immediately after FUS (FUS, n=4), after P-gp inhibition using
 7 tariquidar (TQD, n=5), 24h after FUS without (FUS+24h, n=5) or with P-gp inhibition (FUS+24h/TQD,
 8 n=5). Data are presented as mean ± S.D. ns, not significant, *** p<0.001, 2-way ANOVA with Tukey's
 9 post-hoc test.

10



11

1 **Fig. 5. Kinetic modeling of [¹¹C]metoclopramide PET data obtained in the sonicated brain**
2 **region to the contralateral volume.** The ratio of brain exposure is expressed as AUCR obtained from
3 0 to 10 min or to 0 – 30 min is shown in A. The uptake transfer constant in the sonicated brain region
4 relative to the contralateral hemisphere, expressed as R_1 , is shown in B. Data were acquired either at
5 baseline (n=5), immediately after FUS (FUS, n=4), after P-gp inhibition using tariquidar (TQD, n=5),
6 24h after FUS without (FUS+24h, n=5) or with P-gp inhibition (FUS+24h/TQD, n=5). Data are
7 presented as mean \pm S.D.

8

9 As expected, P-gp inhibition in the absence of FUS (TQD group) significantly increased the
10 brain exposure of [¹¹C]metoclopramide (+135.0 \pm 12.9% in AUC_{30min} p<0.05, Fig. 4) relative to
11 the baseline but did not impact AUCR, suggesting a similar level of P-gp inhibition at the BBB
12 in both the right and left hemispheres (Fig. 5). Brain exposure (AUC_{10min} and AUC_{30min}) of
13 [¹¹C]metoclopramide in the sonicated hemisphere of the FUS+24h/TQD was significantly
14 higher compared with either the baseline group (p<0.05) or the FUS+24h group (p<0.05),
15 most likely due to P-gp inhibition in the whole brain. However, in the FUS+24h/TQD group,
16 AUCR_{10min} was significantly higher compared with all other tested groups, suggesting higher
17 initial brain uptake in the sonicated volume compared with the non-sonicated hemisphere
18 (Fig. 5A). Kinetic modelling using the SRTM confirmed that the ratio of the uptake clearance
19 relative to the contralateral hemisphere (R_1) was significantly higher in the FUS+24h/TQD
20 group compared with the baseline (+29.1 \pm 15.4%, p<0.001) and all other tested groups
21 (p<0.001, Fig. 5B). However, the overall brain exposure ratio of [¹¹C]metoclopramide
22 (AUCR_{30min}) was not significantly higher in the FUS+24h/TQD group compared with the other
23 groups (p>0.05).

24

25

1 Discussion

2
3 The interplay between the P-gp-mediated efflux, which forms a “functional” barrier, and the
4 “physical” integrity of the BBB remains poorly understood. In the present study, the
5 immediate and delayed impact of FUS-induced BBB disruption on P-gp function was
6 investigated in rats. To this end, [¹¹C]metoclopramide PET imaging was performed
7 immediately after FUS-induced BBB disruption, as well as 24h after FUS, at time point when
8 a significant down-regulation of P-gp expression at the BBB was observed.

9 The FUS protocol used in this study has been specifically designed to estimate the impact of
10 BBB disruption upon BBB function using minimally-invasive PET imaging [21]. The size of
11 the brain volume with disrupted BBB is consistent with the spatial resolution of PET scanner
12 (~1.6 mm) and allows for quantification and comparison with the contralateral hemisphere,
13 where the BBB is intact. Similar FUS conditions were applied in mice and were shown to
14 enhance the brain delivery of [¹⁸F]fluoro-desoxy-sorbitol ([¹⁸F]FDS) as a quantitative PET
15 probe for BBB permeability [23]. The EB extravasation test was systematically performed at
16 the end of PET acquisition to inform on the integrity status of the BBB during PET
17 acquisition. No EB extravasation was observed 24h after FUS, suggesting recovery of the
18 paracellular integrity BBB at this time point, consistent with the previously described
19 dynamics of BBB recovery following FUS [34]. It should be noticed that FUS also enables
20 drug delivery to the brain through the stimulation of caveolae-mediated transcytosis which
21 residual activity may still exist 24h after FUS [35–37].

22 The present results, obtained in rats using [¹¹C]metoclopramide as a model P-gp substrate,
23 do not support the use FUS-induced BBB disruption to deliver drugs whose brain penetration
24 is selectively limited by P-gp rather than the physical BBB integrity. This is consistent with
25 previous work performed using similar FUS and PET conditions for [¹¹C]erlotinib, which is a
26 dual substrate of P-gp and the Breast Cancer Resistance Protein (BCRP), and the avid P-gp
27 substrate [¹¹C]N-desmethyl-loperamide [21]. As a consequence, efflux transporters may still
28 restrict drug delivery to the brain, even when physical BBB integrity is lost, as observed for
29 some P-gp substrates in animal models of brain tumors [38]. The combination of FUS-
30 induced BBB disruption with partial P-gp inhibition was not tested for [¹¹C]metoclopramide.
31 However, in this previous study, FUS did not improve the brain delivery of [¹¹C]erlotinib when
32 P-gp and BCRP were inhibited [21]. From a drug delivery perspective, P-gp inhibition
33 increases exposure of [¹¹C]metoclopramide in the whole brain, so that the added value of
34 FUS to enable targeted brain delivery would be lost compared with clinically validated
35 protocols enabling almost complete P-gp inhibition [39].

36 Of note, metoclopramide is a weak substrate of the P-gp, which means it shows substantial
37 brain penetration even when P-gp is fully functional. Moreover, it was shown that

1 [¹¹C]metoclopramide freely crosses the BBB when P-gp inhibited [26,40]. This is consistent
2 with the high passive diffusion of metoclopramide across artificial lipid membrane [41]. This
3 may explain the negligible impact of FUS on the brain delivery of [¹¹C]metoclopramide. Our
4 data suggest that the CNS adverse effects observed in some patients treated with
5 metoclopramide as an antiemetic drug [42] are not likely to be related to a loss in BBB
6 integrity. CNS adverse effects may however be linked to increased plasma exposure and/or
7 enhanced brain distribution which may be caused by impaired P-gp function at the BBB.

8 We hypothesized that the regional decrease in P-gp expression observed at 24h after FUS
9 by several groups [17–19] may provide an innovative mean to locally enhance the brain
10 delivery of P-gp substrates in selected brain regions. So far, pharmacological inhibition of P-
11 gp at the BBB using tariquidar was shown feasible in animals and humans, as highlighted by
12 previous PET studies using radiolabeled substrates of this transporter like (*R*)-[¹¹C]verapamil
13 [39] or [¹¹C]*N*-desmethyl-loperamide [43,44]. However, pharmacological inhibition occurs in
14 the whole-brain [45] which does not allow for targeted brain delivery of P-gp substrates.
15 Fluorescence microscopy on immunostained brain sections confirmed a regional decrease in
16 P-gp expression in the sonicated region, which was maximal at 24h after FUS, a time point at
17 which BBB integrity had already recovered in terms of paracellular transport, according to the
18 absence of EB extravasation. It should, however, be noticed that only a partial -45%
19 decrease in P-gp expression was achieved. This result is consistent with previous studies
20 reporting a significant but partial down-regulation of P-gp at the BBB from 24h to 48h after
21 FUS [17–20]. These studies used different acoustic pressure and FUS conditions. Cho et al.
22 reported an inverse correlation between the level of FUS-induced BBB disruption and the
23 down-regulation of P-gp [17]. Aryal et al. have shown that the maximum level of P-gp
24 suppression was correlated with harmonic emission rather than acoustic pressure [18].
25 However, it remains to be demonstrated whether FUS conditions may be further optimized to
26 lead to more pronounced decrease in P-gp expression, with the aim to approach complete
27 down-regulation.

28 [¹¹C]metoclopramide was selected over previous PET radiotracers for P-gp because it was
29 demonstrated to be more sensitive to assess partial inhibition of the P-gp, suggesting high
30 sensitivity to detect moderate changes in P-gp function at the BBB [26]. Contrary to our
31 expectations, the brain uptake of [¹¹C]metoclopramide was not increased in the sonicated
32 brain volume in the FUS+24h group. Neither was the brain uptake of [¹¹C]metoclopramide
33 relative to the contralateral, non-sonicated hemisphere increased. This observation supports
34 the nonlinear hypothesis assuming that nearly maximal P-gp inhibition or depletion is
35 required to substantially enhance the brain delivery of substrates [46]. This is consistent with
36 previous study reporting that the brain uptake of (*R*)-[¹¹C]verapamil or [¹¹C]*N*-desmethyl-
37 loperamide was not increased in heterozygous *Abcb1a/b*^(+/-) mice expressing 50% less P-gp

1 at the BBB compared with wild-type mice [47], **although, species differences in terms of P-gp**
2 **abundance at the BBB between rats and mice should be considered [48,49].**

3 From an imaging perspective, this suggests that decrease in P-gp function observed in
4 elderly subjects or patients with Alzheimer's disease using PET is probably associated with
5 high degree of decline in P-gp expression at the BBB [50,51]. A correlation of PET data
6 obtained *in vivo* with P-gp expression measured *ex vivo* in resected brain samples would be
7 of interest to estimate the level of P-gp expression associated with a change in the brain
8 kinetics of P-gp PET probes.

9 We further hypothesized that partial inhibition of the P-gp using tariquidar may enhance the
10 brain delivery of [¹¹C]metoclopramide in the presence of the ~45% down-regulation of P-gp
11 expression induced by FUS, leading to an additive effect. Partial P-gp inhibition was
12 previously reported to enhance the sensitivity of (*R*)-[¹¹C]verapamil PET imaging to detect a
13 partial decrease in P-gp function at the BBB [52,53]. The tariquidar dose selected in this work
14 (1 mg/kg) was shown to inhibit 50% of the total P-gp function in rats [26]. Tariquidar, at dose
15 up to 8 mg/kg was shown to not impact the arterial input function of [¹¹C]metoclopramide. In
16 the absence of FUS, tariquidar induced a significant 2.3-fold increase in the brain distribution
17 of [¹¹C]metoclopramide, which extent was the same in both hemispheres. However, when
18 PET imaging under conditions of partial P-gp inhibition with tariquidar was performed 24h
19 after FUS (FUS+24h/TQD group), a significant 11.1±4.4% increase in the initial brain uptake
20 of [¹¹C]metoclopramide relative to the contralateral hemisphere (AUCR_{10 min}) was measured.
21 This effect was not observed in the absence of tariquidar (FUS+24h group, -1.7±2.1%
22 change in AUCR_{10min}), which indicated that partial inhibition using tariquidar significantly
23 enhanced the sensitivity of [¹¹C]metoclopramide PET to detect this moderate and regional
24 decline in P-gp function induced by FUS. However, overall brain exposure of
25 [¹¹C]metoclopramide (AUC_{30 min}) in the sonicated brain volume of the FUS+24h/TQD group
26 was not higher than that observed in the TQD group. This does not support a possible
27 exploitation of the delayed impact of FUS on P-gp expression as a strategy to locally
28 enhance the brain delivery of P-gp substrates for therapeutic purposes.

29 Kinetic modeling was useful to interpret the dynamic PET data obtained with
30 [¹¹C]metoclopramide in the FUS+24h/TQD group. First, a difference between the sonicated
31 and the contralateral hemisphere was observed in the initial uptake phase only (AUCR_{10min}).
32 Consistently, the kinetic parameter R₁, which corresponds to the ratio of the brain delivery in
33 a targeted regions relative to a reference region estimated using the SRTM model [33], was
34 also increased in the FUS+24h/TQD group compared with all other groups. **This is consistent**
35 **with the local down-regulation of P-gp expression. It may also be hypothesized that the**
36 **increase in R₁ observed 24h after FUS may reflect residual stimulation of the caveolae-**
37 **mediated transcytosis, which was not evaluated using the EB extravasation test [35–37].**

1 However, the increase in R_1 was only observed in the presence of partial P-gp inhibition, but
2 not in the FUS nor the FUS+24h group. This supports a link between decreased R_1 and the
3 local P-gp down-regulation.

4 However, a significant increase in the initial brain uptake ($AUCR_{10min}$ and R_1) did not translate
5 into a significant increase in the overall brain exposure (AUC_{30min} and $AUCR_{30min}$) compared
6 with the FUS+24h group. It may be hypothesized that [^{11}C]metoclopramide may preferentially
7 penetrate the brain in the sonicated volume due to decreased P-gp function, and then diffuse
8 to the rest of the brain, where P-gp is normally active, according to the “bulk-flow” hypothesis
9 [54]. Accordingly, a local decrease in P-gp function may not appear as a relevant strategy
10 compared with pharmacological inhibition to enable the brain exposure to P-gp substrates.

11 PET imaging using radiolabeled substrates is widely used to investigate P-gp dysfunction in
12 many pathophysiological conditions [55,56]. However, concurrent changes in both the
13 physical integrity of the BBB and P-gp function can be observed in pathological conditions
14 [55]. Our results obtained in rats suggests that quantification of P-gp function using
15 [^{11}C]metoclopramide may not depend on the integrity status of the BBB. This supports the
16 use of [^{11}C]metoclopramide PET imaging to evaluate P-gp in neurological diseases in which
17 a loss in BBB integrity is suspected [57].

18 The results obtained in the present study should be carefully interpreted in terms of clinical
19 translation and safety consideration for clinical use. Proteomic studies have notably shown
20 large species differences in terms of abundance of efflux transporters at the BBB, with a ~10-
21 fold higher expression of P-gp in rats compared with humans [58]. Consistently, almost
22 complete inhibition of P-gp using tariquidar led to a 3.5-fold increase in the brain uptake of
23 [^{11}C]metoclopramide in rats [25], and a 2.0-fold increase in non-human primates [40] which
24 BBB more closely resembles that of humans in terms of P-gp expression [59]. This suggests
25 that the rat model may overestimate the relative importance of P-gp in limiting the brain
26 uptake of [^{11}C]metoclopramide in humans [48]. Taking advantage of the translational
27 potential of [^{11}C]metoclopramide PET imaging [29,40], further experiments should be
28 conducted in nonhuman primates or humans to confirm the present preclinical results in a
29 perspective of clinical safety.

30

31 **Conclusion**

32 In rats, BBB disruption induced by FUS did not impact the brain kinetics of
33 [^{11}C]metoclopramide, a PET probe for P-gp function at the BBB. [^{11}C]Metoclopramide, under
34 conditions of partial P-gp inhibition, has the sensitivity to detect the functional impact of a
35 moderate decline in P-gp expression observed 24h after FUS. However, this moderate and
36 regional decline in P-gp expression did not translate into a substantial increase in brain
37 exposure. This rat study suggests that almost complete down-regulation of P-gp expression

1 is **probably** required to substantially enhance the brain delivery of compounds which brain
2 distribution is predominantly impaired by the P-gp-mediated efflux rather than physical BBB
3 integrity. **This PET data should however be confirmed in humans given important species**
4 **differences between humans and rodents in terms of P-gp abundance at the BBB.**

6 **Acknowledgements**

7 We gratefully thank Maud Goislard for technical assistance.

10 **Grant support**

11 This work was performed on a platform member of France Life Imaging network (grant ANR-
12 11-INBS-0006).

15 **References**

- 16 1. Banks WA. From blood–brain barrier to blood–brain interface: new opportunities for CNS
17 drug delivery. *Nat Rev Drug Discov.* 2016;15:275–92.
- 18 2. Abbott NJ, Patabendige AAK, Dolman DEM, Yusof SR, Begley DJ. Structure and function
19 of the blood-brain barrier. *Neurobiol Dis.* 2010;37:13–25.
- 20 3. De Bock M, Van Haver V, Vandembroucke RE, Decrock E, Wang N, Leybaert L. Into
21 rather unexplored terrain—transcellular transport across the blood–brain barrier. *Glia.*
22 2016;64:1097–123.
- 23 4. Ronaldson PT, Davis TP. Transport Mechanisms at the Blood-Brain Barrier and in Cellular
24 Compartments of the Neurovascular Unit: Focus on CNS Delivery of Small Molecule Drugs.
25 *Pharmaceutics.* 2022;14:1501.
- 26 5. Durmus S, Hendriks JJMA, Schinkel AH. Apical ABC transporters and cancer
27 chemotherapeutic drug disposition. *Adv Cancer Res.* 2015;125:1–41.
- 28 6. Pathan N, Shende P. Tailoring of P-glycoprotein for effective transportation of actives
29 across blood-brain-barrier. *J Controlled Release.* 2021;335:398–407.
- 30 7. Miyama T, Takanaga H, Matsuo H, Yamano K, Yamamoto K, Iga T, et al. P-Glycoprotein-
31 Mediated Transport of Itraconazole across the Blood-Brain Barrier. *Antimicrob Agents*
32 *Chemother.* 1998;42:1738–44.
- 33 8. Agrawal N, Rowe J, Lan J, Yu Q, Hrycyna CA, Chmielewski J. Potential Tools for
34 Eradicating HIV Reservoirs in the Brain: Development of Trojan Horse Prodrugs for the
35 Inhibition of P-Glycoprotein with Anti-HIV-1 Activity. *J Med Chem.* 2020;63:2131–8.
- 36 9. Kemper EM, Boogerd W, Thuis I, Beijnen JH, van Tellingen O. Modulation of the blood-
37 brain barrier in oncology: therapeutic opportunities for the treatment of brain tumours?
38 *Cancer Treat Rev.* 2004;30:415–23.
- 39 10. Pardridge WM. The Blood-Brain Barrier: Bottleneck in Brain Drug Development.
40 *NeuroRx.* 2005;2:3–14.
- 41 11. de Lange ECM, Hammarlund Udenaes M. Understanding the Blood-Brain Barrier and
42 Beyond: Challenges and Opportunities for Novel CNS Therapeutics. *Clin Pharmacol Ther.*
43 2022;111:758–73.
- 44 12. Cox B, Nicolai J, Williamson B. The role of the efflux transporter, P-glycoprotein, at the
45 blood–brain barrier in drug discovery. *Biopharm Drug Dispos.* 2023;44:113–26.

- 1 13. Couture O, Foley J, Kassell NF, Larrat B, Aubry J-F. Review of ultrasound mediated drug
2 delivery for cancer treatment: updates from pre-clinical studies. *Transl Cancer Res.*
3 2014;3:494–511.
- 4 14. Gorick CM, Breza VR, Nowak KM, Cheng VWT, Fisher DG, Debski AC, et al.
5 Applications of focused ultrasound-mediated blood-brain barrier opening. *Adv Drug Deliv*
6 *Rev.* 2022;191:114583.
- 7 15. Mittapalli RK, Manda VK, Bohn KA, Adkins CE, Lockman PR. Quantitative
8 fluorescence microscopy provides high resolution imaging of passive diffusion and P-gp
9 mediated efflux at the in vivo blood-brain barrier. *J Neurosci Methods.* 2013;219:188–95.
- 10 16. Adkins CE, Mittapalli RK, Manda VK, Nounou MI, Mohammad AS, Terrell TB, et al. P-
11 glycoprotein mediated efflux limits substrate and drug uptake in a preclinical brain metastases
12 of breast cancer model. *Front Pharmacol.* 2013;4:136.
- 13 17. Cho H, Lee H-Y, Han M, Choi J-R, Ahn S, Lee T, et al. Localized Down-regulation of P-
14 glycoprotein by Focused Ultrasound and Microbubbles induced Blood-Brain Barrier
15 Disruption in Rat Brain. *Sci Rep.* 2016;6:31201.
- 16 18. Aryal M, Fischer K, Gentile C, Gitto S, Zhang Y-Z, McDannold N. Effects on P-
17 Glycoprotein Expression after Blood-Brain Barrier Disruption Using Focused Ultrasound and
18 Microbubbles. *PloS One.* 2017;12:e0166061.
- 19 19. Choi H, Lee E-H, Han M, An S-H, Park J. Diminished Expression of P-glycoprotein
20 Using Focused Ultrasound Is Associated With JNK-Dependent Signaling Pathway in Cerebral
21 Blood Vessels. *Front Neurosci.* 2019;13:1350.
- 22 20. Conti A, Geffroy F, Kamimura HAS, Novell A, Tournier N, Mériaux S, et al. Regulation
23 of P-glycoprotein and Breast Cancer Resistance Protein Expression Induced by Focused
24 Ultrasound-Mediated Blood-Brain Barrier Disruption: A Pilot Study. *Int J Mol Sci.*
25 2022;23:15488.
- 26 21. Goutal S, Gerstenmayer M, Auvity S, Caillé F, Mériaux S, Buvat I, et al. Physical blood-
27 brain barrier disruption induced by focused ultrasound does not overcome the transporter-
28 mediated efflux of erlotinib. *J Controlled Release.* 2018;292:210–20.
- 29 22. Arif WM, Elsinga PH, Gasca-Salas C, Versluis M, Martínez-Fernández R, Dierckx RAJO,
30 et al. Focused ultrasound for opening blood-brain barrier and drug delivery monitored with
31 positron emission tomography. *J Controlled Release.* 2020;324:303–16.
- 32 23. Hugon G, Goutal S, Dauba A, Breuil L, Larrat B, Winkeler A, et al. [18F]2-Fluoro-2-
33 deoxy-sorbitol PET Imaging for Quantitative Monitoring of Enhanced Blood-Brain Barrier
34 Permeability Induced by Focused Ultrasound. *Pharmaceutics.* 2021;13:1752.
- 35 24. Tran VL, Novell A, Tournier N, Gerstenmayer M, Schweitzer-Chaput A, Mateos C, et al.
36 Impact of blood-brain barrier permeabilization induced by ultrasound associated to
37 microbubbles on the brain delivery and kinetics of cetuximab: An immunoPET study using
38 ⁸⁹Zr-cetuximab. *J Controlled Release.* 2020;328:304–12.
- 39 25. Pottier G, Marie S, Goutal S, Auvity S, Peyronneau M-A, Stute S, et al. Imaging the
40 Impact of the P-Glycoprotein (ABCB1) Function on the Brain Kinetics of Metoclopramide. *J*
41 *Nucl Med.* 2016;57:309–14.
- 42 26. Breuil L, Marie S, Goutal S, Auvity S, Truillet C, Saba W, et al. Comparative
43 vulnerability of PET radioligands to partial inhibition of P-glycoprotein at the blood-brain
44 barrier: A criterion of choice? *J Cereb Blood Flow Metab.* 2022;42:175–85.
- 45 27. Breuil L, Goutal S, Marie S, Del Vecchio A, Audisio D, Soyer A, et al. Comparison of the
46 Blood-Brain Barrier Transport and Vulnerability to P-Glycoprotein-Mediated Drug-Drug
47 Interaction of Domperidone versus Metoclopramide Assessed Using In Vitro Assay and PET
48 Imaging. *Pharmaceutics.* 2022;14:1658.
- 49 28. Zoufal V, Mairinger S, Brackhan M, Krohn M, Filip T, Sauberer M, et al. Imaging P-
50 Glycoprotein Induction at the Blood-Brain Barrier of a β -Amyloidosis Mouse Model with

1 11C-Metoclopramide PET. *J Nucl Med.* 2020;61:1050–7.
2 29. Tournier N, Bauer M, Pichler V, Nics L, Klebermass E-M, Bamminger K, et al. Impact of
3 P-Glycoprotein Function on the Brain Kinetics of the Weak Substrate 11C-Metoclopramide
4 Assessed with PET Imaging in Humans. *J Nucl Med.* 2019;60:985–91.
5 30. Caillé F, Goutal S, Marie S, Auvity S, Cisternino S, Kuhnast, Bertrand, et al. PET
6 imaging reveals a saturable liver uptake transport of importance for the pharmacokinetics of
7 metoclopramide. *Contrast Media Mol Imaging.* In Press. 2018;In Press.
8 31. Gerstenmayer M, Fellah B, Magnin R, Selingue E, Larrat B. Acoustic Transmission
9 Factor through the Rat Skull as a Function of Body Mass, Frequency and Position. *Ultrasound*
10 *Med Biol.* 2018;44:2336–44.
11 32. Schneider CA, Rasband WS, Eliceiri KW. NIH Image to ImageJ: 25 years of image
12 analysis. *Nat Methods.* 2012;9:671–5.
13 33. Lammertsma AA, Hume SP. Simplified reference tissue model for PET receptor studies.
14 *NeuroImage.* 1996;4:153–8.
15 34. Marty B, Larrat B, Van Landeghem M, Robic C, Robert P, Port M, et al. Dynamic Study
16 of Blood–Brain Barrier Closure after its Disruption using Ultrasound: A Quantitative
17 Analysis. *J Cereb Blood Flow Metab.* 2012;32:1948–58.
18 35. Meng Y, Pople CB, Lea-Banks H, Abrahao A, Davidson B, Suppiah S, et al. Safety and
19 efficacy of focused ultrasound induced blood-brain barrier opening, an integrative review of
20 animal and human studies. *J Controlled Release.* 2019;309:25–36.
21 36. Olsman M, Sereti V, Mühlenpfordt M, Johnsen KB, Andresen TL, Urquhart AJ, et al.
22 Focused Ultrasound and Microbubble Treatment Increases Delivery of Transferrin Receptor-
23 Targeting Liposomes to the Brain. *Ultrasound Med Biol.* 2021;47:1343–55.
24 37. Pandit R, Koh WK, Sullivan RKP, Palliyaguru T, Parton RG, Götz J. Role for caveolin-
25 mediated transcytosis in facilitating transport of large cargoes into the brain via ultrasound. *J*
26 *Controlled Release.* 2020;327:667–75.
27 38. de Gooijer MC, Kemper EM, Buil LCM, Çitirikkaya CH, Buckle T, Beijnen JH, et al.
28 ATP-binding cassette transporters restrict drug delivery and efficacy against brain tumors
29 even when blood-brain barrier integrity is lost. *Cell Rep Med.* 2021;2:100184.
30 39. Bauer M, Karch R, Zeitlinger M, Philippe C, Römermann K, Stanek J, et al. Approaching
31 complete inhibition of P-glycoprotein at the human blood-brain barrier: an (R)-
32 [11C]verapamil PET study. *J Cereb Blood Flow Metab.* 2015;35:743–6.
33 40. Auvity S, Caillé F, Marie S, Wimberley C, Bauer M, Langer O, et al. P-Glycoprotein
34 (ABCB1) Inhibits the Influx and Increases the Efflux of 11C-Metoclopramide Across the
35 Blood-Brain Barrier: A PET Study on Nonhuman Primates. *J Nucl Med.* 2018;59:1609–15.
36 41. Tsinman O, Tsinman K, Sun N, Avdeef A. Physicochemical Selectivity of the BBB
37 Microenvironment Governing Passive Diffusion—Matching with a Porcine Brain Lipid
38 Extract Artificial Membrane Permeability Model. *Pharm Res.* 2011;28:337–63.
39 42. Parkman HP, Mishra A, Jacobs M, Pathikonda M, Sachdeva P, Gaughan J, et al. Clinical
40 response and side effects of metoclopramide: associations with clinical, demographic, and
41 pharmacogenetic parameters. *J Clin Gastroenterol.* 2012;46:494–503.
42 43. Langer O. Use of PET Imaging to Evaluate Transporter-Mediated Drug-Drug Interactions.
43 *J Clin Pharmacol.* 2016;56 Suppl 7:S143-156.
44 44. Kreisl WC, Bhatia R, Morse CL, Woock AE, Zoghbi SS, Shetty HU, et al. Increased
45 permeability-glycoprotein inhibition at the human blood-brain barrier can be safely achieved
46 by performing PET during peak plasma concentrations of tariquidar. *J Nucl Med.*
47 2015;56:82–7.
48 45. Eyal S, Ke B, Muzi M, Link JM, Mankoff DA, Collier AC, et al. Regional P-glycoprotein
49 activity and inhibition at the human blood-brain barrier as imaged by positron emission
50 tomography. *Clin Pharmacol Ther.* 2010;87:579–85.

- 1 46. Kalvass JC, Polli JW, Bourdet DL, Feng B, Huang S-M, Liu X, et al. Why clinical
2 modulation of efflux transport at the human blood-brain barrier is unlikely: the ITC evidence-
3 based position. *Clin Pharmacol Ther.* 2013;94:80–94.
- 4 47. Wanek T, Römermann K, Mairinger S, Stanek J, Sauberer M, Filip T, et al. Factors
5 Governing P-Glycoprotein-Mediated Drug-Drug Interactions at the Blood-Brain Barrier
6 Measured with Positron Emission Tomography. *Mol Pharm.* 2015;12:3214–25.
- 7 48. Verscheijden LFM, Koenderink JB, de Wildt SN, Russel FGM. Differences in P-
8 glycoprotein activity in human and rodent blood–brain barrier assessed by mechanistic
9 modelling. *Arch Toxicol.* 2021;95:3015–29.
- 10 49. Zhang W, Liu QY, Haqqani AS, Liu Z, Sodja C, Leclerc S, et al. Differential Expression
11 of ABC Transporter Genes in Brain Vessels vs. Peripheral Tissues and Vessels from Human,
12 Mouse and Rat. *Pharmaceutics.* 2023;15:1563.
- 13 50. Deo AK, Borson S, Link JM, Domino K, Eary JF, Ke B, et al. Activity of P-Glycoprotein,
14 a β -Amyloid Transporter at the Blood-Brain Barrier, Is Compromised in Patients with Mild
15 Alzheimer Disease. *J Nucl Med.* 2014;55:1106–11.
- 16 51. Bauer M, Bamminger K, Pichler V, Weber M, Binder S, Maier-Salamon A, et al.
17 Impaired clearance from the brain increases the brain exposure to metoclopramide in elderly
18 subjects. *Clin Pharmacol Ther.* 2020;
- 19 52. Bauer M, Wulkersdorfer B, Karch R, Philippe C, Jäger W, Stanek J, et al. Effect of P-
20 glycoprotein inhibition at the blood–brain barrier on brain distribution of (R)-[11C]verapamil
21 in elderly vs. young subjects. *Br J Clin Pharmacol.* 2017;83:1991–9.
- 22 53. Zoufal V, Wanek T, Krohn M, Mairinger S, Filip T, Sauberer M, et al. Age dependency of
23 cerebral P-glycoprotein function in wild-type and APPPS1 mice measured with PET. *J Cereb*
24 *Blood Flow Metab.* 2020;40:150–62.
- 25 54. Groothuis DR, Vavra MW, Schlageter KE, Kang EW-Y, Itskovich AC, Hertzler S, et al.
26 Efflux of drugs and solutes from brain: the interactive roles of diffusional transcapillary
27 transport, bulk flow and capillary transporters. *J Cereb Blood Flow Metab.* 2007;27:43–56.
- 28 55. Gil-Martins E, Barbosa DJ, Silva V, Remião F, Silva R. Dysfunction of ABC transporters
29 at the blood-brain barrier: Role in neurological disorders. *Pharmacol Ther.* 2020;213:107554.
- 30 56. Harris WJ, Asselin M-C, Hinz R, Parkes LM, Allan S, Schiessl I, et al. In vivo methods
31 for imaging blood-brain barrier function and dysfunction. *Eur J Nucl Med Mol Imaging.*
32 2022;
- 33 57. Obermeier B, Daneman R, Ransohoff RM. Development, maintenance and disruption of
34 the blood-brain barrier. *Nat Med.* 2013;19:1584–96.
- 35 58. Uchida Y, Yagi Y, Takao M, Tano M, Umetsu M, Hirano S, et al. Comparison of
36 Absolute Protein Abundances of Transporters and Receptors among Blood-Brain Barriers at
37 Different Cerebral Regions and the Blood-Spinal Cord Barrier in Humans and Rats. *Mol*
38 *Pharm.* 2020;17:2006–20.
- 39 59. Uchida Y, Wakayama K, Ohtsuki S, Chiba M, Ohe T, Ishii Y, et al. Blood-brain barrier
40 pharmacoproteomics-based reconstruction of the in vivo brain distribution of P-glycoprotein
41 substrates in cynomolgus monkeys. *J Pharmacol Exp Ther.* 2014;350:578–88.
- 42